ECS Journal of Solid State Science and Technology, **3** (8) R164-R167 (2014)
2162-8769/2014/3(8)/R164/4/$31.00 © The Electrochemical Society

Formation of Recombination Zone in Blue Phosphorescent Organic Light-Emitting Diodes with Different Electron Transport Layers and Its Effects on Device Performance

Sang Ho Rhee,[a] Yong-Min Lee,[a] Ki Won Kim,[a] Chang Su Kim,[b] Myungkwan Song,[b] Kwun-Bum Chung,[c] Sung Hyun Kim,[d,z] and Seung Yoon Ryu[a,z]

[a]*Department of Information Display, Sunmoon University, Sunmoon-ro, Tangjeong-myeon, Asan, Chungnam, 336-708, Korea*
[b]*Advanced Functional Thin Films Department, Korea Institute of Materials Science (KIMS), 797 Changwondaero, Seongsangu, Changwon 641-831, Korea*
[c]*Division of Physics and Semiconductor Science, Dongguk University, Seoul, 100-715, Korea*
[d]*Department of Chemistry, College of Natural Sciences, Seoul National University, Seoul 151-747, Korea*

The effects of the electron mobilities and energy levels of different electron transport layer (ETL) materials on the performances were systemically investigated in blue phosphorescent organic light-emitting diodes. The spatial control of recombination zone (RZ) which was accompanied with triplet exciton quenching affected the balance between holes and electrons in the emission layer, resulting in the variations of the device performances. An optical micro-cavity effect in the electroluminescence (EL) spectrum around 500 nm was noticed by employing tris(8-hydroxyquinolinolato)aluminum (Alq_3) ETL. This was attributed to the broadening of the emission zone through the emission layer over the ETL, exhibiting the greenish color coordinates. The current efficiency of the device with 3-phenyl-4(10-naphthyl)-5-phenyl-1,2,4-triazole (TAZ) ETL was much higher than that of the same structured device with any other ETL due to better charge balance as well as the suppression of triplet exciton quenching by the narrow RZ with low electron mobility and proper band alignment.

Manuscript submitted May 16, 2014; revised manuscript received July 10, 2014. Published July 18, 2014.

Organic light-emitting diodes (OLEDs)[1–10] are believed to open the next generation display and illumination, owing to their highly desirable properties, which can be used to fabricate ultra-thin, high resolution, flexible, and transparent displays for large-scale mass production at low costs through simple processes. Generally, it is thought that phosphorescent OLEDs (PHOLEDs) are showing the higher quantum efficiency than that of fluorescent OLEDs by four times through the use of both singlet and triplet excitons.[1–10]

Theoretically, red and green PHOLEDs have almost achieved 20% external quantum efficiency by confining excitons and charges within an emission layer (EML).[1–10] However, in spite of the development of noble organic materials and device structure, there are a number of issues related to the use of blue PHOLEDs such as low device efficiency and poor long-term stability.[1–10] One of most challenging issues is triplet exciton quenching, that is generated in a recombination zone (RZ) of the EML or at the interface between the EML and hole transport layer (HTL)/electron transport layer (ETL). Then, they can be easily diffused to its adjacent layers and quenched because the triplet energy of carrier transport layers is lower than that of EML. Therefore, the charge transport layers such as HTL and ETL should have higher triplet energy than that of phosphorescent host and dopant for the suppression of triplet exciton quenching.

In general, many researchers have used iridium-(III) bis-[(4,6-difluorophenyl)-pyridinato-N,$C^{2'}$] picolinate (FIrpic) as a dopant and *N,N′*-dicarbazolyl-3,5-benzene (mCP) as a host for blue PHOLEDs.[3] Assuming *N,N*-bis-(1-naphthyl)-*N,N′*-diphenyl-1,1′-biphenyl-4,4′diamine (NPB) is employed as a HTL, triplet exciton energy is transferred from the EML to the HTL because of lower triplet bandgap of NPB (2.3 eV) than that of FIrpic (2.7 eV) and mCP (2.9 eV).[3,4,13] The diffusion length of triplet exitons can be reached up to 100 nm compared with 10 nm of singlet excitons due to the long excited state lifetime of μs order.[2,16] Triplet excitons are formed at the interface between HTL and EML, and diffused into NPB, finally quenched. Therefore, the proper selection of charge transporting material with corresponding mobility with NPB HTL is very important for improving device performance which is affected by triplet exciton quenching in the device.

A number of studies have investigated the effect of ETL materials such as 3-phenyl-4(10-naphthyl)-5-phenyl-1,2,4-triazole (TAZ)[4] and tris(8-hydroxyquinolinolato)aluminum (Alq_3),[5–7] which have low electron transport mobility, and 2,9-dimethyl-4,7-diphenyl-1,10-phenanthroline (BPhen)[6,10] and 2-[3,5-bis(1-phenylbenzimidazol-2-yl)phenyl]-1-phenylbenzimidazole (TPBi),[7] which show high electron mobility in the device. Utilizing the appropriate mobility of ETL with proper energy barrier can improve the charge balance in the RZ, resulting in the enhanced efficiency and desirable color coordinates in PHOLEDs.[8,9,13] Especially, Tang and Chen et al. have revealed that the size of RZ was critically related to carrier mobility, the higher mobility induced the wider RZ, resulting the electroluminescence (EL) peak change.[7,9] That means the formation of RZ is critically related the carrier mobility, including electron mobility of ETL. In this study, we investigated the correlation between the formation of RZ and the device performance according to the different ETL materials in blue phosphorescent devices.

Experimental

Following the process used for fabricating conventional OLEDs, first indium tin oxide (ITO) glass was treated by deionized water, acetone, and isopropanol, under sonication. It was then subjected to an ultraviolet-ozone (UVO) treatment to remove any residual organics and to increase the ITO work function.[11,12] 1,4,5,8,9,11-hexaazatriphenylene-hexacarbonitrile (HAT-CN) (60 nm) and NPB (30 nm) was used as a hole injection layer (HIL) and a HTL. mCP doped with 10% FIrpic was used as the EML (20 nm) and subsequent mCP was used for the exciton blocking layer (EBL) (5 nm). Alq_3, TAZ, TPBi, or BPhen was deposited for ETL (20 nm). Finally, LiF/Al (1 nm/130 nm) was used as cathode system. Each layer was thermally deposited in a high-vacuum chamber using a shadow mask with an area of 4 mm^2. We refer to the device according to the ETL such as TAZ as "TAZ device", Alq_3 as "Alq_3 device", BPhen as "BPhen device", and TPBi as "TPBi device".

The current density-luminance-voltage characteristics and the electroluminescence (EL) spectra of the devices were respectively obtained using a Keithley 2400 voltmeter and a Minolta CS-1000 spectrometer, respectively.

Results and Discussion

Figures 1 shows the device configuration and energy level diagram for the blue PHOLEDs fabricated with different ETL materials. The

[z]E-mail: shkim75@snu.ac.kr; justie74@sunmoon.ac.kr

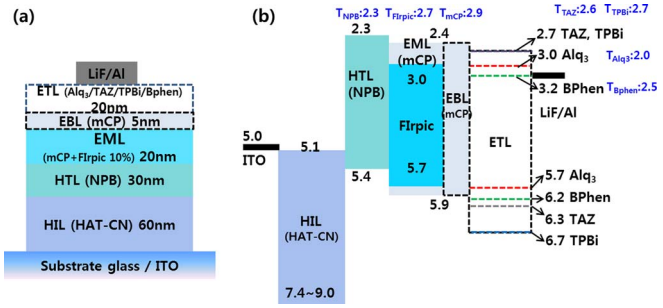

Figure 1. (a) Device structure and (b) energy level diagrams depending on the different ETL in PHOLEDs. [T_A = triplet energy level for A].

triplet bandgaps of the various layers are 2.3 eV for NPB, 2.9 eV for mCP, 2.7 eV for FIrpic, 2.6 eV for TAZ, 2.0 for Alq_3, 2.5 eV for BPhen, 2.7 eV for TPBi, respectively.[4–7,10] It has been reported that HAT-CN as a HIL exhibited a significant increase in the current density, which give rise to a higher luminance, current efficiency, and power efficiency.[18,19] The Fermi-level of HAT-CN is almost closed to lowest unoccupied molecular orbital (LUMO) and holes and electrons move through Fermi-level like metallic property, showing quite high electron mobility of 2.9×10^{-2} cm^2/V s.[18,19] Thus, the band alignment is well-matched with ITO and NPB. However, too high carrier mobility of HAT-CN could not be beneficial for charge balance in EML. The EBL made of mCP can prevent the diffusion of triplet excitons from EML into ETL.[3,13,14]

In the energy band diagram, the triplet excitons could be formed at the interface between the HTL and the EML, and diffused to NPB, finally quenched because the triplet energy of NPB (2.3 eV) is smaller than that of FIrpic (2.6 eV).[3,10] Hole accumulation between the EML and the ETL in all devices was facilitated by the large energy barrier except the device using Alq_3 ETL, while meaningful electron accumulation was occurred at the interface between the ETL and the EML in the device with BPhen ETL.[6,10] The location of the exciton formation and the degree of triplet exciton quenching was varied with the different ETL which exhibited different charge injection and transport capability.

Fig. 2 shows the current densities and electron mobilities of the different ETL materials, calculated by the space-charge limited current (SCLC) method for electron-only devices (EODs).[23–28] The configuration of the EODs was as following; ITO/LiF (3 nm)/ETL (100 nm)/LiF (1.0 nm)/Al (100 nm). The mobilities were field-independent at low voltage and electric field, which is around $8 \sim 10$ V and $5.9 \sim 7.4 \times 10^{-7}$ V/m, respectively.[23–28] while a abrupt increase at high voltage was determined by Mott-Gurney law, fitting the current

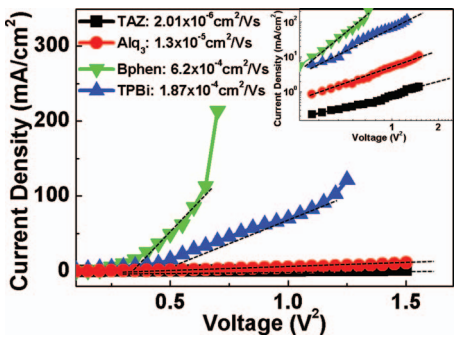

Figure 2. Current densities and calculated electron mobility of the different ETL materials in electron only devices [Inset:log(current density)-log(voltage) curve for the mobility calculation from SCLC fitting].

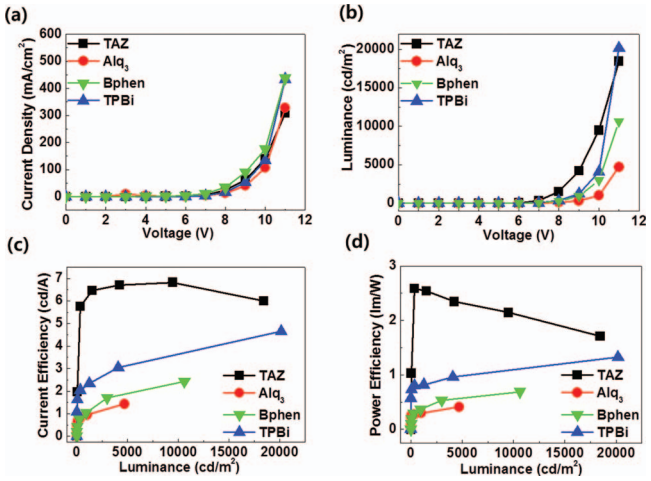

Figure 3. Device performances of the various PHOLEDs; (a) current density vs voltage, (b) luminance vs voltage, (c) current efficiency vs luminance, and (d) power efficiency vs luminance.

density to the model of a single carrier SCLC as presented as[23–28]

$$J = \frac{9}{8}\varepsilon_0\varepsilon_r\mu_0\frac{V^2}{L^3}$$

where J is the current density, μ_0 is the zero-field mobility, ε_0 is the permittivity of free space, ε_r is the relative permittivity of the material and regarded to be 3 for organic materials. L is the thickness of the organic layer and V is the applied voltage.[23–28] Of the four ETL investigated, BPhen showed a highest electron mobility of 6.2 $\times 10^{-4}$ cm^2/V s. The mobilities of TAZ and Alq_3 were significantly lower than those of BPhen and TPBi, while that of Alq_3 was one order of magnitude higher than that of TAZ. We could divide the ETL materials into two categories as those that showed low mobilities (TAZ and Alq_3) and those that exhibited high electron mobilities (BPhen and TPBi). The electron mobilities of the ETL materials could determine triplet exciton formation and quenching, and their performances of corresponding devices.

The current density-voltage, luminance-voltage, current efficiency-luminance and power efficiency-luminance characteristics of the four PHOLEDs with different ETL are shown in Figs. 3a, 3b, 3c, and 3d, respectively. The structure of the four devices was consisted of ITO/HATCN (60 nm)/NPB (30 nm)/mCP: FIrpic (20 nm;10%)/mCP (5 nm)/ETL (20 nm)/LiF (1.0 nm)/Al (130 nm).

The current densities of all four devices are similar in Fig. 3a. The small distinction can be ascribed to the differences in their electron mobilities and to the energy levels of the highest occupied molecular orbital (HOMO) and LUMO. In case of TAZ device, the energy level of LUMO for TAZ is as same as that of TPBi but the HOMO level difference between mCP EBL and TAZ is 0.4 eV, compared to 0.8 eV between EBL and TPBi. However, the current density of TPBi device was higher than that of TAZ device at high voltage due to higher electron mobility of TPBi. Actually, the current density is not exactly related to single parameter, such as the mobility of ETL. It depends on the electron mobility including conductivity, the energy level difference with adjacent layers, the polarity of each layer, and so on. Nevertheless, the lower current density of TAZ device, which was attributed to its low electron mobility, increased the recombination probability between holes and electrons in the EML. This result was found to the increase in the luminance in TAZ device in Fig. 3b. Unlike TAZ device, the luminescence of Alq_3 device was lower than that noticed in other devices. This can be speculated to the fact that the RZ of Alq_3 device was combined with the ETL because the singlet excitons emission of Alq_3 affected the greenish color coordinates of (0.252, 0.442) as shown in Fig. 4b. That means the triplet excitons in EML of Alq_3 device were mixed with the singlet excitons from Alq_3

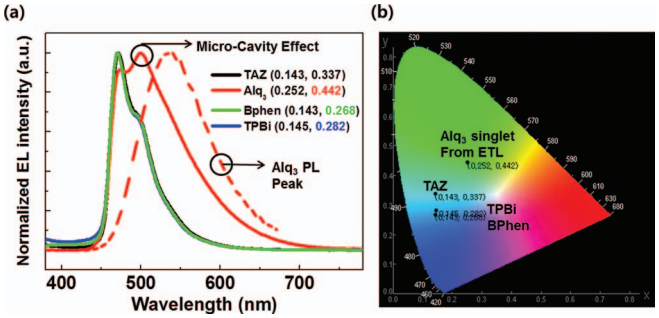

Figure 4. (a) Normalized electroluminescence spectra of the PHOLEDs with different ETL. (b) The CIE color coordinates of various ETL devices. Only Alq_3 device showed the greenish color coordinate of (0.252, 0.442), which means the RZ of Alq_3 device was combined with Alq_3 ETL.

ETL, formed larger RZ and resulted in strong micro-cavity effect. In the ETL, the recombination between holes from EBL and electrons from the cathode is readily facilitated by no hole injection barrier at the interface between EBL and ETL (Fig. 5b). This result was also consistent with the EL spectrum of the device in Fig. 4a. The current and power efficiency of TAZ device was the highest among the values of four different devices. This result was believed that the spatial control of RZ improved the charge balance in EML and reduced a significantly degree of triplet exciton diffusion which consisted of triplet-triplet annihilation (TTA) and triplet-polaron annihilation (TPA).[20–22] In BPhen and TPBi devices, the higher electron mobility of the ETL materials generated triplet excitons at the interface between the HTL and the EML, and diffused to NPB, finally quenched.[7,9] In this device structure, fast electron mobility of ETL is not beneficial for device performance by wider RZ.[7,9] The efficiency of BPhen device is less than that of TPBi device due to the highest electron mobility and the less probability of charge carrier recombination. This, in turn, was because much more triplet excitons were formed at the interface, and diffused to NPB, much more quenched, compared to the suppressed triplet quenching in TPBi device (Fig. 5).

The normalized electroluminescence (EL) spectra and Commission Internationale de l'Eclairage (CIE) color coordinates are shown in Fig. 4a and 4b, respectively. The blue dopant FIrpic is known to exhibit EL peaks at 475 and 500 nm in the literature.[4,10] All devices except Alq_3 device showed typical FIrpic emission peaks, indicating efficient energy transfer from the host to the dopant in the blue PHOLEDs. In the EL spectrum of Alq_3 device, a red-shift as well as an increase in the intensity of the peak around 500 nm was observed due to the micro-cavity effect, which increases the CIE y-coordinate of 0.442 compared to that of 0.337 in TAZ. The photoluminescence (PL) peak of Alq_3 and the color coordinate exhibiting the greenish color are clear reasons why the red-shift in EL spectrum of Alq_3 device was happened, and is the strong evidence for Alq_3 singlet exciton from ETL as shown in Fig. 4a and 4b, respectively. The triplet exciton from mCP:FIrpic and singlet from Alq_3 ETL were obviously combined and formed wide RZ between EML and ETL as shown in Fig. 5b.

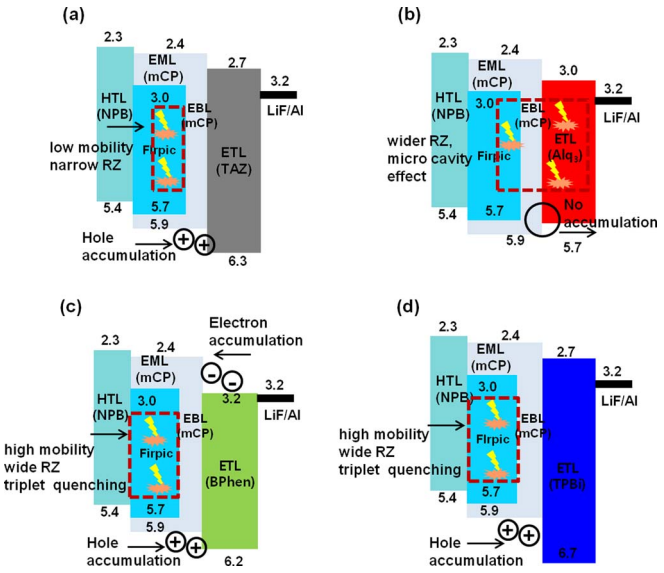

Figure 5. Schematic diagram of charge transport in the devices based on the different ETL as (a) TAZ, (b) Alq_3, (c) BPhen, and (d) TPBi.

The BPhen and TPBi devices showed quite similar color coordinate due to similar RZ size by similar electron mobility, compared to that of TAZ device which showed different CIE y-coordinate due to narrow RZ size by lower electron mobility as shown in Fig. 4b.[7,9] The longer optical path length from the wider RZ and the singlet emission of Alq_3 was found to be the reason for decreased efficiency in Alq_3 device. Therefore, the micro-cavity effect should be prevented for the appropriate value of blue CIE y-coordinate as well as high efficiency.

It is important to confine excitons to the RZ in order to improve the current efficiency in PHOLEDs, which is accompanied by the control of RZ location[8,9,14] and corresponding triplet exciton quenching with TTA and TPA.[20–22] The RZ in the device is affected by many factors, such as energy barrier at the interface, the motilities of charge, and so on.[7,9] The ETL should have functions such as hole blocking to prohibit the overflow of holes into the ETL, utilizing electron mobility and energy levels to increase the charge balance efficiently. The device performance in this study can be determined by the selection of the ETL materials with their properties. This hypothesis is consistent with the experimental results, suggesting that TAZ device has the highest efficiency compared to other devices.

Fig. 5 illustrates the energy level diagrams depending on the various ETL materials. A large difference in the HOMO levels between the EBL and the ETL acts as hole blocking, leading to the hole accumulation at the interface in Fig. 5a, 5c, and 5d. With regard to the experimental results, the narrow RZ of TAZ device is formed close to the EBL, compared to the wider RZ of TPBi and BPhen devices, which can be attributed to the low electron mobility in Fig. 5a.[7,9] However, the RZ of Alq_3 device was localized over ETL, as shown in Fig. 5b, because there was no hole injection barrier between EBL and ETL. This results in singlet exciton emission from the Alq_3 ETL, which induced a micro-cavity effect.[15–17] In addition, the broader RZ affects the CIEy color coordinates mainly.

The RZ of BPhen and TPBi devices are wider than that of TAZ device with respect to their higher electron mobility, which raises the triplet exciton quenching by its long diffusion lengths of (50 nm $\sim$ 100 nm),[2] resulting in the decrease of the efficiency. The efficiency of BPhen device is lower than that of TPBi device, which can be attributed to the higher degree of triplet exciton quenching due to the higher mobility as well as less energy barrier (0.3 eV) between the ETL and the EBL.

Obviously, the RZ in the device could be related with energy barrier at the interface, the motilities of charge and so many factors. However, mainly considering electron mobility of ETL, there could be definite correlation between the device performance and the variation of RZ by electron mobility control.

Conclusions

In summary, we investigated the characteristics of ETL materials, their device performances with the formation of the RZ, and CIE color coordinates of the emission from the resulting PHOLEDs. TAZ device exhibited higher efficiency than other devices due to lower electron mobility, better charge balance, and suppression of triplet exciton quenching. The size of RZ was controlled by the electron mobility in the ETL material and energy barrier at the interface. Although the current density of Alq_3 device was similar to that of TAZ device, Alq_3 device showed lower efficiency and red-shift CIE coordinates due to

the broad RZ over ETL. In addition, the device based on the ETL materials with high electron mobilities (BPhen and TPBi) showed lower efficiencies and wider RZ because the high electron mobility induced the triplet exciton generation at the interface between HTL and EML, diffusion to NPB, and quenching. Finally, we could determine the relationship between the size of RZ and electron mobilities of the ETL materials with different energy levels, and the device performance with color coordinates in the Blue PHOLEDs, which lead an alternative device design for efficient, deep-blue device in practical applications.

Acknowledgments

This research was partially supported by Basic Science Research Program through the National Research Foundation of Korea (NRF) funded by the Ministry of Education, Science and Technology (NRF-2013R1A1A2A10005186). Authors also gratefully acknowledge support from the Pioneer Research Center Program (2013M3C1A3065525) through the National Research Foundation of Korea funded by the Ministry of Science, ICT & Future Planning and the IT R&D Program (no.10042412) funded by Ministry of Trade, Industry, & Energy/Korea Evaluation Institute of Industrial Technology (MOTIE/KEIT, Korea).

References

1. H. Sasabe, J. Takamatsu, T. Motoyama, S. Watanabe, G. Wagenblast, N. Langer, O. Molt, E. Fuchs, C. Lennartz, and J. Kido, *Adv. Mater.*, **22**, 5003 (2010).
2. K. S. Yook and J. Y. Lee, *Adv. Mater.*, **24**, 3169 (2012).
3. R. J. Holmes, S. R. Forrest, Y. J. Tung, R. C. Kwong, J. J. Brown, S. Garon, and M. E. Thompson, *Appl. Phys. Lett.*, **82**, 2422 (2003).
4. Q. Wang, J. Ding, D. Ma, Y. Cheng, L. Wang, X. Jing, and F. Wang, *Adv. Fun. Mater.*, **19**, 84 (2009).
5. S. O. Jeon, K. S. Yook, C. W. Joo, and J. Y. Lee, *Appl. Phys. Lett.*, **94**, 013301 (2009).
6. J. G. Jang, H. J. Ji, H. S. Kim, and J. C. Jeong, *Curr. Appl. Phys.*, **11**, S251 (2011).
7. S. H. Rhee, K. B. Nam, C. S. Kim, and S. Y. Ryu, *Electronchem. solid State Lett.*, **3**, R7 (2014).
8. J. H. Lee, J. I. Lee, J. Y. Lee, and H. Y. Chu, *Appl. Phys. Lett.*, **95**, 253304 (2009).
9. S. W. Culligan, A. C.-A. Chen, J. U. Wallace, K. P. Klubek, C. W. Tang, and S. H. Chen, *Adv. Fun. Mater.*, **16**, 1481 (2006).
10. J. H. Lee, J. I. Lee, K. I. Song, S. J. Lee, and H. Y. Chu, *Appl. Phys. Lett.*, **92**, 133304 (2008).
11. H. K. Lee, J. K. Kim, and O. O. Park, *Org. Electron.*, **10**, 1641 (2009).
12. I. M. Chan, T. Y. Hsu, and F. C. Hong, *Appl. Phys. Lett.*, **81**, 1899 (2002).
13. S. H. Kim, J. Jang, and J. Y. Lee, *Appl. Phys. Lett.*, **90**, 223505 (2007)
14. Y. Zheng, S. Eom, N. Chopra, J. Lee, F. So, and J. Xue, *Appl. Phys. Lett.*, **92**, 223301 (2008).
15. P. E. Burrows, S. R. Forrest, S. P. Sibley, and M. E. Thompson, *Appl. Phys. Lett.*, **69**, 2959 (1996).
16. V. Bulovic, V. B. Khalfin, G. Gu, P. E. Burrows, D. Z. Garbuzov, and S. R. Forrest, *Phys. Rev. B*, **58**, 3730 (1998).
17. C.-J. Lee, Y-I. Park, J.-H. Kwon, and J.-W Park, *Bull. Korean. Chem. Soc.*, **26**, 1344 (2005).
18. S. H. Cho, S. W. Pyo, and M. C. Suh, *Synth. Met.*, **162**, 402 (2012).
19. Y. K. Kim, J. W. Kim, and Y. S. Park, *Appl. Phys. Lett.*, **94**, 063305 (2009).
20. S. Reineke, K. Walzer, and K. Leo, *Phys. Rev. B*, **75**, 125328 (2007).
21. S.-J. Su, T. Chiba, T. Takeda, and J. Kido, *Adv. Mater.*, **20**, 2125 (2008).
22. S. Jeong, M.-K. Kim, S. H. Kim, and J.-I. Hong, *Org. Electron.*, **14**, 2497 (2013).
23. M. A. Lampert and P. Mark, *Current Injection in Solids*, Academic Press, New York (1970).
24. M. Kiy, P. Losio, I. Biaggio, M. Koehler, A. Tapponnier, and P. Gunter, *Appl. Phys. Lett.*, **80**, 1198 (2002).
25. C. G. Zhen, Y. F. Dai, W. J. Zeng, Z. Ma, Z. K. Chen, and J. Kieffer, *Adv. Fun. Mater.*, **21**, 699 (2011).
26. C. Melzer, E. J. Koop, V. D. Mihailetchi, and P. W. M. Blom, *Adv. Fun. Mater.*, **14**, 865 (2004).
27. P. W. M. Blom, C. Tanase, D. M. de Leeuw, and R. Coehoom, *Appl. Phys. Lett.*, **86**, 092105 (2005).
28. Z. He, C. Zhong, X. Huang, W. Y. Wong, H. Wu, L. Chen, S. Su, and Y. Cao, *Adv. Mater.*, **23**, 4636 (2011).